

Determination of optical constants and temperature dependent band gap energy of GaS_{0.25}Se_{0.75} single crystals

M. ISIK^{a*}, N. GASANLY^{b,c}

^aDepartment of Electrical and Electronics Engineering, Atilim University, 06836, Ankara, Turkey

^bDepartment of Physics, Middle East Technical University, 06800, Ankara, Turkey

^cVirtual International Scientific Research Centre, Baku State University, 1148, Baku, Azerbaijan

Optical properties of GaS_{0.25}Se_{0.75} single crystals were investigated by means of temperature-dependent transmission and room temperature reflection experiments. Derivative spectrophotometry analysis showed that indirect band gap energies of the crystal increase from 2.13 to 2.26 eV as temperature is decreased from 300 to 10 K. Temperature dependence of band gap energy was fitted under the light of theoretical expression. The band gap energy change with temperature and absolute zero value of the band gap energy were found from the analyses. The Wemple-DiDomenico single effective oscillator model and Sellmeier oscillator model were applied to the spectral dependence of room temperature refractive index to find optical parameters of the GaS_{0.25}Se_{0.75} crystal. Chemical composition of the crystal was determined using the energy dispersive spectral measurements.

(Received October 20, 2016; accepted June 7, 2017)

Keywords: Semiconductors, Band gap energy, Refractive index

1. Introduction

A^{III}B^{VI} type semiconducting materials, GaSe and GaS, have been attractive compounds due to their beneficial properties to be used in optoelectronic applications. The potential usability of these compounds in optoelectronic devices operating in red and blue visible regions takes the attention of researchers studying on related areas [1-3]. The investigations of these crystals indicated that GaSe is favorable material used in different applications such as nonlinear optical [4], far-infrared conversion [5], second harmonic generation [6], middle infrared [7], terahertz generation [8] and heterostructure devices [9] whereas GaS interests for near blue light emitting devices [10]. A recent work also revealed the potential usability of GaSe/GaS as ultrathin layer transistors [11].

GaSe and GaS crystals form GaS_xSe_{1-x} ($0 \leq x \leq 1$) mixed crystals having distinctive optical and electrical properties in comparison to the end compounds. Under the light of technological importance of GaSe and GaS crystals, GaS_xSe_{1-x} mixed crystals can be thought as potential candidates for fabrication of long-pass filter, light emitting devices and optical detecting systems. Previously, optical properties of GaS_xSe_{1-x} and its constituents GaSe and GaS were investigated in many studies. Optical characterization techniques performed on GaSe and GaS resulted in indirect band gap energies of 1.988 and 2.55 eV, respectively [12, 13]. The variation of band gap energy with composition was investigated for GaS_xSe_{1-x} mixed crystals ($0 \leq x \leq 0.5$) using transmission and piezoreflectance measurements [13]. It was revealed that band gap energies of the mixed crystals increases from 1.99 eV ($x = 0$) to 2.37 eV ($x = 0.5$). Real defect structure, physical properties and optical quality of GaS_xSe_{1-x} crystals were presented using transmittance

electron microscopy, reflection, high energy electron diffraction and selected area electron diffraction [14, 15]. GaS_xSe_{1-x} crystals were also investigated using ellipsometry measurements in the composition range of $0 \leq x \leq 1$ [16]. The interband transition energies and their change with composition were also reported in the relevant paper. Four interband transition structures were obtained in crystals corresponding to $x = 0.3$ which is the most similar one through the studied crystals to GaS_{0.25}Se_{0.75} which is the interest of the present work.

The present paper is aimed at the investigation of the optical parameters of GaS_{0.25}Se_{0.75} ($x = 0.25$) crystals, one of the members of GaS_xSe_{1-x} mixed crystals, using temperature-dependent transmission and room temperature reflection experiments. The band gap energy, refractive index spectra, absolute zero value of the band gap energy, rate of change of band gap energy with temperature are some of the revealed optical properties in the present study. Furthermore, Wemple-DiDomenico single effective oscillator model and Sellmeier oscillator model were used to expand optical researches on the studied crystal and obtain oscillator energy and strength, dispersion energy, zero frequency dielectric constant and refractive index.

2. Experimental details

GaS_{0.25}Se_{0.75} polycrystals were synthesized using high-purity elements (at least 99.999%) prepared in stoichiometric proportions. Single crystals were grown by the Bridgman method in evacuated (10^{-5} Torr) silica tubes (10 mm in diameter and about 25 cm in length) with a tip at the bottom in our crystal growth laboratory. The ampoule was moved in a vertical furnace through a thermal gradient

of 30 °C/cm, between the temperatures 1000 and 650 °C at a rate of 0.5 mm/h. The resulting ingots were easily cleaved along the planes that are perpendicular to the *c*-axis of the crystal. The determination of the chemical composition of the crystal was performed using the energy dispersive spectral (EDS) analysis experiments. The experiments were performed using JSM-6400 scanning electron microscope.

Transmission and reflection measurements were carried out in the 400–1000 nm spectral range using Shimadzu UV 1201 model spectrophotometer with resolution of 5 nm, which is equipped by a 20 W halogen lamp, a holographic grating and a silicon photodiode. Transmission measurements were performed under normal incidence of light with a polarization direction along the (001) plane. This plane is perpendicular to the *c*-axis of the crystal. For the reflection experiments, a specular reflectance measurement attachment with a 5° incident angle was used. Temperature-dependent transmission measurements were performed in the 10–300 K range using Advanced Research Systems, Model CSW-202 closed cycle helium cryostat to cool the sample. The accuracy of the cooling system was 0.5 K. Reflection experiments were only accomplished at room temperature since technical problems related to usage of cryostat did not allow us to perform the experiments at low temperatures.

3. Results and discussion

Fig. 1 shows the EDS spectra of GaS_{0.25}Se_{0.75} crystal, as recorded to determine the chemical composition of the samples. The characteristics emission energies for Ga, S and Se elements are (1.098, 1.125, 1.144, 1.171 and 9.241 keV), (0.163, 0.164, 2.307, 2.464 and 2.470 keV) and (1.379, 1.419, 1.434 and 1.475 keV), respectively [17]. EDS analyses resulted in atomic composition of (Ga : Se : S) as (50.4 : 12.2 : 37.4). This compositional relation is well matched with nominal composition of *x* = 0.25.

The temperature dependence of transmittance (*T*) and room temperature reflectance (*R*) spectra are presented in Fig. 2. The plotted figures in the present work are concentrated on the region in which analyses were done and absorption takes place although the measurements were performed in the 400–1000 nm spectral range. The room temperature reflection measurements were carried out using samples with natural cleavage planes and thickness (*d*) such that $ad \gg 1$ where *a* symbolizes the absorption coefficient. Thickness of the used crystal for transmission experiments was calculated using [18]

$$d = \frac{1}{2n} \left(\frac{\lambda_1 \lambda_2}{\lambda_2 - \lambda_1} \right) \quad (1)$$

where λ_1 and λ_2 are wavelengths of maximum intensity positions of two neighboring transmission interference fringes in the transmittance spectra. The thickness of the thin samples was calculated using Eq. (1) nearly as 18 μm. In the literature, there are different analytic techniques used to find the band gap energy from transmittance and reflectance spectra. Derivative spectrophotometry is one of

these techniques using the maxima and minima positions of the derivative curve to determine the band gap energy [19].

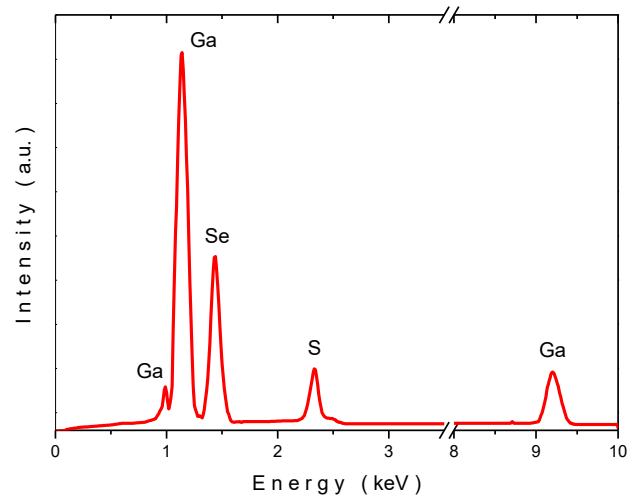


Fig. 1. Energy dispersive spectroscopic analysis of GaS_{0.25}Se_{0.75} mixed crystals

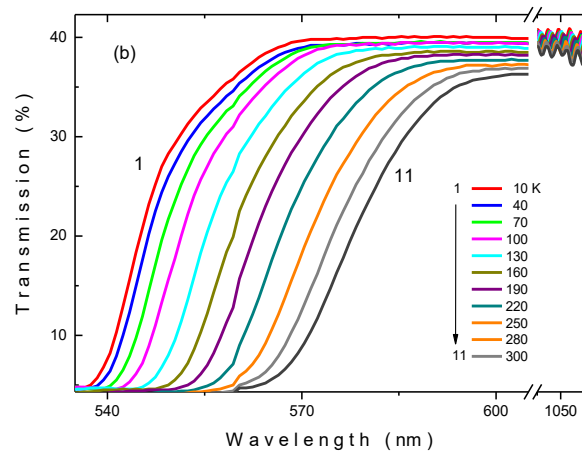
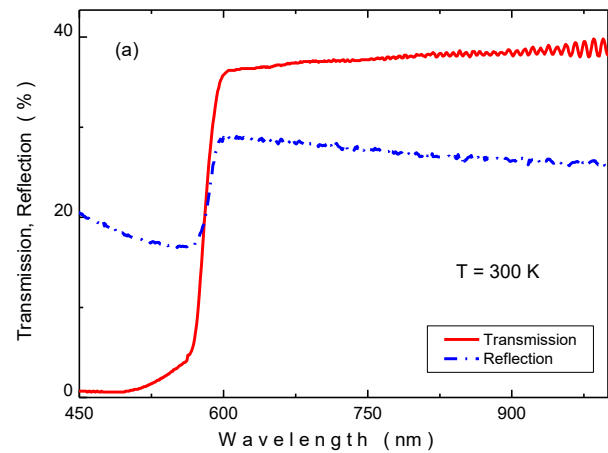


Fig. 2. The spectral dependences of the (a) transmittance and the reflectance at room temperature (b) transmittance at different temperatures of GaS_{0.25}Se_{0.75} mixed crystals

Fig. 3 and its inset show the first derivatives of temperature dependent transmittance and room temperature reflectance spectra, respectively. The spectra of $dT/d\lambda$ and $dR/d\lambda$ at room temperature exhibit peaks at energies of 2.13 and 2.14 eV, respectively, corresponding to band gap energies of the $\text{GaS}_{0.25}\text{Se}_{0.75}$ crystal. The temperature-dependent spectra of $dT/d\lambda$ results in band gap energies increasing from 2.13 to 2.27 eV as the temperature decreases from 300 to 10 K (see Fig. 4). The band gap energy variation with composition in $\text{GaS}_x\text{Se}_{1-x}$ mixed crystals was fitted by the expression of $E(x) = E(0) + bx + cx^2$ [13]. According to the fitting parameters, the band gap energy of $\text{GaS}_{0.25}\text{Se}_{0.75}$ crystal was estimated as 2.16 eV which shows a good agreement with our revealed value of 2.13 eV. The derivative analysis of the absorption coefficient was also used to find the band gap energy. The relation between absorption coefficient and photon energy is given by the expression [20]

$$\frac{d \ln(\alpha h\nu)}{d(h\nu)} = \frac{p}{h\nu - E_g} \quad (2)$$

This equation indicates that $d(\ln(\alpha h\nu))/d(h\nu)$ vs. $(h\nu)$ plot presents a peak when $h\nu$ is equal to E_g . Figure 5 shows the corresponding plot which exhibits a peak at 2.15 eV. Absorption coefficient can be used to get Urbach energy associated with structural disorder and defects within the crystal. The theoretical expression called as Urbach rule for this purpose is [21]

$$\alpha = \alpha_0 \exp[h\nu / E_u] \quad (3)$$

where α_0 and E_u symbolize the characteristic crystal parameter and Urbach energy, respectively. As can be concluded from Eq.(3), the slope of $\ln(\alpha)$ vs. $h\nu$ plot can be utilized to find the Urbach energy. The inset in Fig. 5 shows the corresponding plot and its linear fit near band edge. The inverse of the slope of fitted line gives the Urbach energy as 52 meV.

Temperature dependence of the band gap energy is expressed by [18]

$$E_g(T) = E_g(0) + \frac{\gamma T^2}{T + \beta} \quad (4)$$

where $E_g(0)$ is absolute zero value of band gap, γ is rate of change of the band gap with temperature and β is Debye temperature. The experimental data (open circles) and fit outcome (solid line) in Fig. 4 show a good consistency for optical parameters of $E_{gi}(0) = 2.27$ eV and $\gamma = -5.3 \times 10^{-4}$ eV/K.

The refractive index spectrum at room temperature (Fig. 6) was plotted using reflectivity (Fig. 2a) and the expression [18]

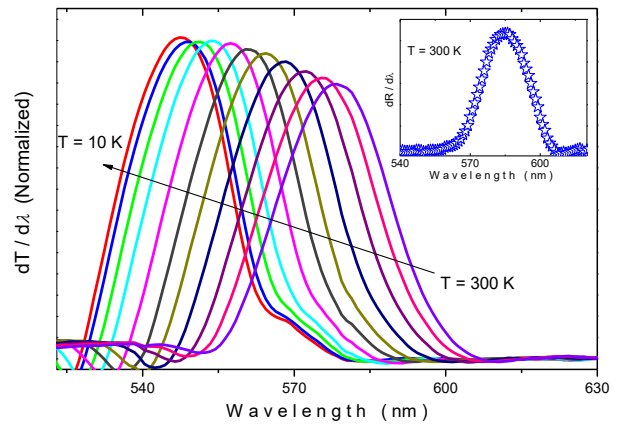


Fig. 3. The spectral dependence of $dT/d\lambda$ at different temperatures. Inset presents the spectral dependence of $dR/d\lambda$ at room temperature for $\text{GaS}_{0.25}\text{Se}_{0.75}$ mixed crystals

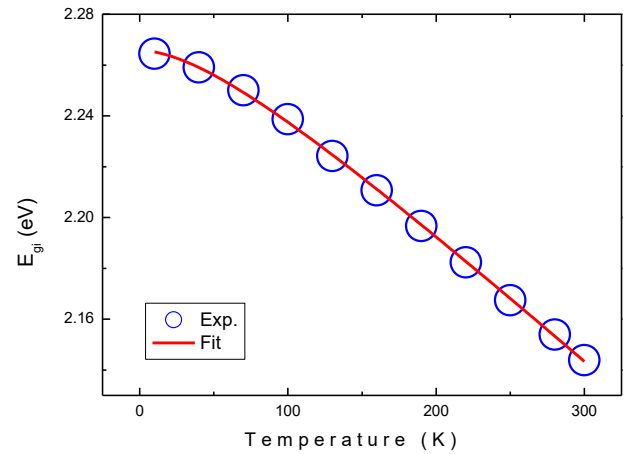


Fig. 4. Temperature dependence of band gap energy of $\text{GaS}_{0.25}\text{Se}_{0.75}$ mixed crystals

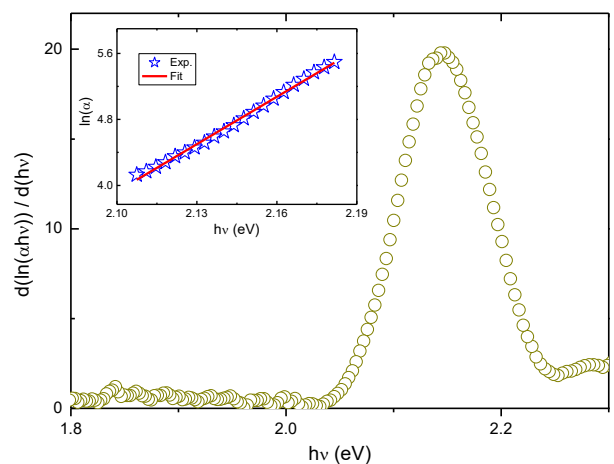


Fig. 5. The dependence of $d(\ln(\alpha h\nu))/d(h\nu)$ on photon energy for $\text{GaS}_{0.25}\text{Se}_{0.75}$ crystal at room temperature. Inset shows the plot of $\ln(\alpha)$ vs. $h\nu$ (stars) and its linear fit (solid line)

$$n = \frac{1+R}{1-R} + \left[\frac{4R}{(1-R^2)} - \left(\frac{\alpha\lambda}{4\pi} \right)^2 \right]^{1/2} \quad (5)$$

As seen from the figure, refractive index decreases slightly with wavelength in the transparent region of 650-1000 nm. However, refractive index decreases rapidly with decreasing wavelength in the resonance energy region of 550-600 nm. This observed extraordinary behavior in the spectrum takes place persistently in the neighborhood of absorption bands in the absorption spectrum. Refractive index values of GaS_xSe_{1-x} mixed crystals were estimated as [22]

$$n^2(\text{GaS}_x\text{Se}_{1-x}) = xn^2(\text{GaS}) + (1-x)n^2(\text{GaSe}) \quad (6)$$

The refractive indices of GaSe and GaS are around 2.83 and 2.65, respectively, in the 800-1000 nm spectral region which is the common range of present and referenced paper. According to Eq. (6), the refractive index of GaS_{0.25}Se_{0.75} crystal is estimated as 2.79 which shows a good consistency with refractive index value of 2.78 picked out from Fig. 6.

Sellmeier oscillator model and single effective oscillator model suggested by Wemple & DiDomenico express the refractive index in the $h\nu < E_g$ region. In the Sellmeier oscillator model, refractive index is related in the $h\nu < E_g$ region by [23]

$$(n^2 - 1)^{-1} = \frac{1}{S_{so}\lambda_{so}^2} - \frac{1}{S_{so}\lambda^2} \quad (7)$$

where S_{so} and λ_{so} symbolize the oscillator strength and wavelength, respectively. Inset of Fig. 6 presents the linear fit of experimental data according to Eq. (7). The linear fit of $(n^2 - 1)^{-1}$ vs. λ^{-2} curve gives the oscillator parameters as $S_{so} = 7.14 \times 10^{13} \text{ m}^{-2}$ and $\lambda_{so} = 2.9 \times 10^{-7} \text{ m}$. In the Wemple-DiDomenico model, photon energy dependence of refractive index is given as [24]

$$n^2(h\nu) = 1 + \frac{E_{so}E_d}{E_{so}^2 - (h\nu)^2} \quad (8)$$

where E_{so} and E_d represents the single oscillator energy and dispersion energy, respectively. E_d is a measure of the strength of the interband optical transition whereas E_{so} is average gap energy. The fitting process resulted in $E_{so} = 4.26 \text{ eV}$ and $E_d = 25.7 \text{ eV}$. The ratio of E_{so}/E_{gi} for GaS_{0.25}Se_{0.75} crystal was obtained as 1.99 which shows a good agreement with relation of $E_{so} \approx 2E_{gi}$ [25, 26].

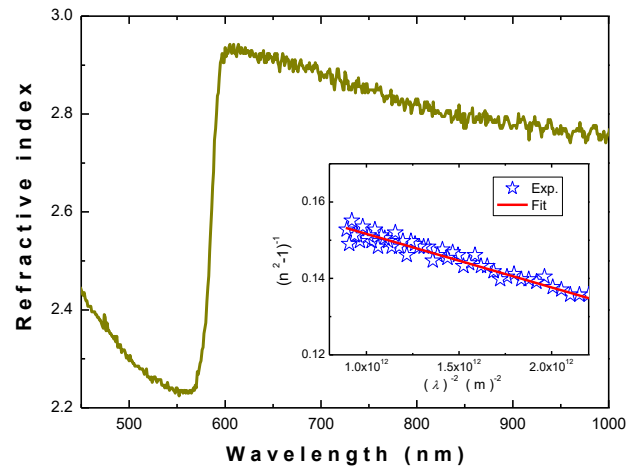


Fig. 6. The variation of refractive index as a function of wavelength at room temperature. Inset: The plot of $(n^2 - 1)^{-1}$ vs. $(\lambda)^{-2}$ in the $h\nu < E_g$ range. Stars are experimental data and solid line represents the linear fit

4. Conclusions

GaS_{0.25}Se_{0.75} semiconducting single crystals were optically investigated using temperature-dependent transmission and room temperature reflection experiments. Temperature and wavelength ranges of the measurements were 10-300 K and 400-1000 nm, respectively. Band gap energy of the crystal was obtained taking advantage of first derivative of transmittance and reflectance spectra. The increase of band gap energy from 2.13 to 2.26 eV with the decrease of temperature from 300 to 10 K was revealed as a result of analyses. The band gap energy change with temperature and absolute band gap energy zero-temperature value were found as $\gamma = -5.3 \times 10^{-4} \text{ eV/K}$ and $E_g(0) = 2.27 \text{ eV}$. Analyses on the spectral dependence of refractive index in the below band gap energy region using Wemple-DiDomenico single effective oscillator model resulted in oscillator energy of 4.26 eV and dispersion energy of 25.7 eV. Sellmeier oscillator model applied in the same region revealed the oscillator strength and wavelength as $9.66 \times 10^{13} \text{ m}^{-2}$ and $2.5 \times 10^{-7} \text{ m}$, respectively.

References

- [1] S. Shigetomi, T. Ikari, H. Nakashima, J. Appl. Phys. **74**, 4125 (1993).
- [2] A. G. Kyazym-zade, R. N. Mekhtieva, A. A. Akhmedov, Sov. Phys. Semicond. **25**, 840 (1991).

- [3] N. B. Singh, D. R. Suhre, V. Balakrishna, M. Marable, R. Meyer, N. Fernelius, F. K. Hopkins, D. Zelmon, *Prog. Cryst. Growth Ch.* **37**, 47 (1998).
- [4] G. Manfredotti, A. Rizzo, A. Bufo, V. L. Cardetta, *Phys. Status Solidi A* **30**, 375 (1975).
- [5] G. Micocci, A. Serra, A. Tepore, *J. Appl. Phys.* **82**, 2365 (1997).
- [6] Z. Feng, Z. Kang, F. Wu, J. Gao, Y. Jiang, H. Zhang, Y. M. Andreev, G. V. Lanskii, V.V. Atuchin, T. A. Gavrilova, *Opt. Express* **16**, 9978 (2008).
- [7] Z. Kang, J. Guo, Z. Feng, J. Gao, J. Xie, L. Zhang, V. Atuchin, Y. Andreev, G. Lanskii, A. Shaiduko, *Appl. Phys. B* **108**, 545 (2012).
- [8] S. A. Bereznyaya, Z. V. Korotchenko, R. A. Redkin, S. Yu. Sarkisov, V. N. Brudnyi, A. V. Kosobutsky, V. V. Atuchin, *Inf. Phys. Technol.* **77**, 100 (2016).
- [9] K. Allakhverdiev, F. Ismailov, L. Kador, M. Braun, *Solid State Commun.* **104**, 1 (1997).
- [10] N. B. Singh, R. Narayanan, A. X. Zhao, V. Balakrishna, R. H. Hopkins, D. R. Suhre, N. C. Fernelius, F. K. Hopkins, D. E. Zelmon, *J. Mater. Sci. Eng. B* **49**, 243 (1997).
- [11] D. J. Late, B. Liu, J. Luo, A. Yan, H. S. S. R. Matte, M. Grayson, C. N. R. Rao, V. P. Dravid, *Adv. Mater.* **24**, 3549 (2012).
- [12] C. H. Ho, S. L. Lin, *J. Appl. Phys.* **100**, 083508 (2006).
- [13] C.C. Wu, C.H. Ho, W.T. Shen, Z. H. Cheng, Y. S. Huang, K. K. Tiong, *Mater. Chem. Phys.* **88**, 313 (2004).
- [14] Yu. M. Andreev, V. V. Atuchin, G. V. Lanskii, A. N. Morozov, L. D. Pokrovsky, S. Yu. Sarkisov, O. V. Voevodina, *Mater. Sci. Eng. B* **128**, 205 (2006).
- [15] K. A. Kokh, V. V. Atuchin, T. A. Gavrilova, A. Kozhukhov, E. A. Maximovskiy, L. D. Pokrovsky, A. R. Tsygankova, A. I. Saprykin, *J. Microscopy* **256**, 208 (2014).
- [16] M. Isik, N. Gasanly, *Opt. Mater.* **54**, 155 (2016).
- [17] J. Goldstein, D. Newbury, D. Joy, C. Lyman, P. Echlin, E. Lifshin, L. Sawyer, J. Michael, *Scanning Electron Microscopy and X-Ray Microanalysis*, Springer Science, LLC, New York, 2007.
- [18] J. I. Pankove, *Optical Processes in Semiconductors*, Prentice-Hall, New Jersey, 1971.
- [19] C. B. Ojeda, F. S. Rojas, *Microchem. J.* **106**, 1 (2013).
- [20] F. Yakuphanoglu, *J. Phys. Chem. Solids* **69**, 949 (2008).
- [21] F. Urbach, *Phys. Rev.* **92**, 1324 (1953).
- [22] J. A. Van Vechten, T.K. Bergstresser, *Phys. Rev. B* **1**, 3351 (1970).
- [23] A. K. Walton, T. S. Moss, *P. Phys. Soc.* **81**, 509 (1963).
- [24] S. H. Wemple, M. DiDomenico, *Phys. Rev. B* **3**, 1338 (1971).
- [25] K. Tanaka, *Thin Solid Films* **66**, 271 (1980).
- [26] F. Yakuphanoglu, A. Cukurovali, I. Yilmaz, *Physica B* **351**, 53 (2004).

*Corresponding author: mehmet.isik@atilim.edu.tr